KfK 4701
Mai 1990

Assessment of the Physico-chemical Properties of Phases in the Na-U-Pu-O System

H. Kleykamp
Institut für Material- und Festkörperforschung
Projekt Nukleare Sicherheitsforschung

Kernforschungszentrum Karlsruhe

KERNFORSCHUNGSZENTRUM KARLSRUHE
Institut für Material- und Festkörperforschung
Projekt Nukleare Sicherheitsforschung

KfK 4701

Assessment of the physico-chemical properties of phases in the Na-U-Pu-O system

H. Kleykamp

Kernforschungszentrum Karlsruhe GmbH, Karlsruhe

Kernforschungszentrum Karlsruhe GmbH
Postfach 3640, 7500 Karlsruhe 1

ISSN 0303-4003

Zusammenstellung der physikalisch-chemischen Eigenschaften der im System Na-U-Pu-O auftretenden Phasen

Zusammenfassung

Die physikalisch-chemischen Eigenschaften der in den Systemen Na-O, Na-U-O, Na-Pu-O und Na-U-Pu-O auftretenden Phasen werden kritisch beurteilt. Die Zusammenstellung beinhaltet die Phasendiagramme sowie die kristallographischen, mechanischen, thermischen, thermodynamischen, Transport-, optischen und chemischen Eigenschaften. Diese Daten sind für die modellmäßige Beschreibung des thermischen, mechanischen und chemischen Verhaltens flüssigmetallgekühlter Mischoxidbrennstäbe für schnelle Brutreaktoren während und nach der Bestrahlung vorgesehen.

Abstract

A critical review is given on the physico-chemical properties of phases in the Na-O, Na-U-O, Na-Pu-O and Na-U-Pu-O systems. This includes the phase diagrams as well as the crystallographic, mechanical, thermal, thermodynamic, transport, optical and chemical properties. This data is to be used for the modelling of the thermal, mechanical and chemical behaviour of defective LMFBR mixed oxide pins during and after reactor operation.

Preface

The present version of this report is an amendment of a draft that had been prepared for the AGT 010101 subgroup on out-of-pile fuel properties. A number of suggestions was made by the members of the subgroup and most recent experimental results were incorporated into this report. Final agreement was attained at the meeting in London on 10 - 11 January 1990 by the members J.P. Piron, Belgonucleaire; Y. Guerin and Y. Philipponneau, CEA/Cadarache; C. Heyne, Interatom; H. Kleykamp, KfK; R.G.J. Ball, J.H. Harding, D.G. Martin, M.A. Mignanelli, P.E. Potter and M.H. Rand, UKAEA/Harwell; J. Edwards and H.M. MacLeod, UKAEA/Windscale. The author of this report gratefully acknowledges the fruitful discussions with Dr. M.A. Mignanelli.

Contents

1. Thermodynamics of the fuel-sodium reactions

The operation of defective uranium-plutonium oxide pins in sodium cooled fast breeder reactors results in chemical reactions between the fuel and the coolant because the system $(U,Pu)O_2$-Na is not in thermodynamic equilibrium. After pin failure the stoichiometric or slightly hypostoichiometric oxide $(U,Pu)O_2$ is in contact with sodium containing about 3 wt.-ppm oxygen that is typical for the sodium loop of a fast breeder reactor. This non-equilibrium is represented in fig. 1 by the dotted line of the schematic isothermal section of the pseudoternary Na-$U_{0.8}Pu_{0.2}$-O system at 1000 K. Reactions between the fuel and sodium occur until the oxygen content of the fuel and of the sodium is adjusted to their equilibrium threshold values. The excess oxygen in the fuel and sodium are used for the formation of the reaction product $Na_3(U,Pu)O_4$ or other sodium uranoplutonates which occur predominantly as layers between the fuel and the coolant on the inside of the pins. The reaction comes to a standstill when the fuel is reduced to a strongly hypostoichiometric composition and is in thermodynamic equilibrium with $Na_3(U,Pu)O_4$ and Na containing dissolved oxygen at the threshold concentration, e.g. 11 wt.-ppm O at 1000K, see three-phase field in fig. 1. The oxygen equilibrium concentration in sodium is far below the maximum oxygen solubility in sodium which is about 6000 wt.-ppm at 1000 K (see table 1).

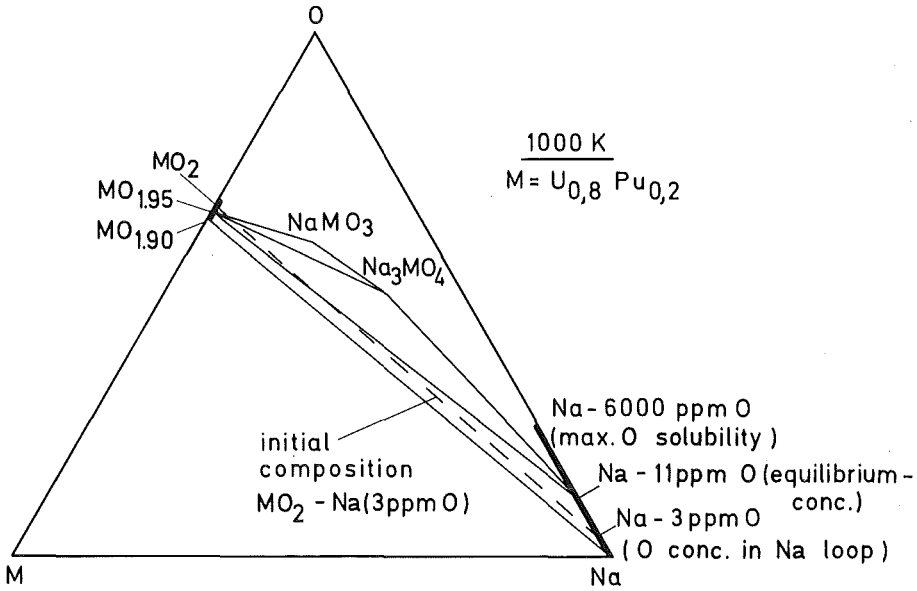

Fig. 1: Schematic isothermal section of the pseudoternary Na-$U_{0.8}Pu_{0.2}$-O system at 1000 K (1 ppm ≙ 1 µg/g).

The outlined isothermal conditions of the closed system are idealized for defective pins because a radial temperature gradient exists in the fuel which involves an oxygen concentration gradient and "fresh" sodium can flow through the defective pins during further reactor operation.

$Na_3(U,Pu)O_4$ is the dominant reaction product which has unfavourable mechanical, thermal and chemical properties for the defective pin behaviour. Most of the properties are unknown. Therefore, it has not been effective to model the mechanical and chemical behaviour of defective fuel pins so far. On the other hand, some physico-chemical properties of Na_3UO_4 are known which are useful information; however, they can be only reservedly accepted to $Na_3(U,Pu)O_4$.

In this paper the physico-chemical data of phases of the systems Na-O, Na-U-O, Na-Pu-O and Na-U-Pu-O are compiled and critically assessed as far as they are necessary for the modelling of defective mixed oxide fuel pins.

2. The Na-O system

The Na-O system is treated here as far as it is of relevance for the Na-U-O, Na-Pu-O and Na-U-Pu-O systems. The solubility region of oxygen in sodium results from the sodium rich part of the Na-O phase diagram in fig. 2 [1]. The temperature dependence of the maximum solubility of oxygen $c_O°$ in sodium was critically evaluated by Noden in 1973 [2] and was confirmed by Maupré in 1978 [1] which gives $\log c_O°$ (wt.-ppm) = 6.257 - 2444.5/T between 377 and 873 K. Further data were obtained from the operation of sodium loops by Thorley [47], the values were cited earlier by Taylor and Thomson [3]: $\log c_O°$ (wt.-ppm) = 5.153 - 1803/T between 387 and 799 K. Numerical data of these two equations [2,3,47] are compiled in table 1 together with the older Eichelberger values in the temperature range 398 - 828 K [42] and Hislop's et al. results [43] measured between 398 and 523 K by gamma activation analysis. As the assessment of Noden also includes the results reviewed by Eichelberger only the expression derived by the former will be used in the later sections. Noden's and Thorley's data are graphically represented in fig. 3. Any preference of these data sets cannot be given at the moment. However, this uncertainty influences the accuracy of the calculated oxygen concentration in sodium in equilibrium with $Na_3(U,Pu)O_4$ and $(U,Pu)O_2$ and with Na_3UO_4 and UO_2, resp., see table 9.

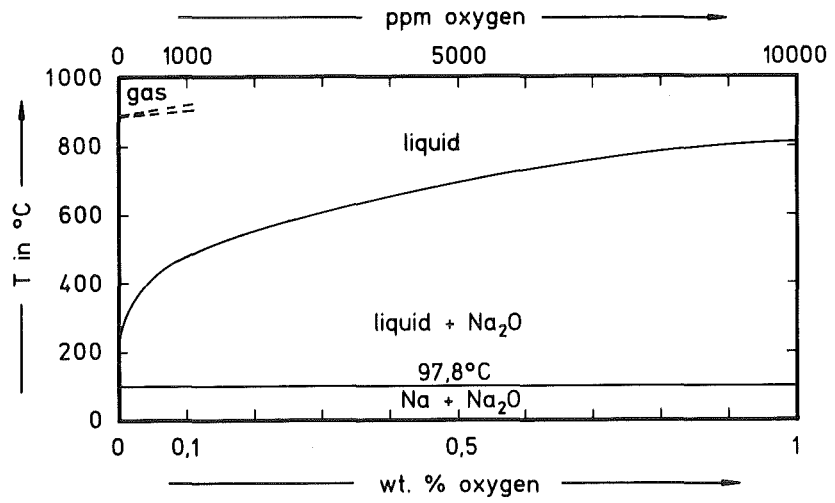

Fig. 2: Sodium side of the phase diagram of the Na-O system.

Table 1: Maximum solubility of oxygen $c_O°$ in sodium.

T in K	$c_O°$ in wt.-ppm oxygen			
	Eichelberger [42]	Noden [2]	Hislop [43]	Thorley [3,47]
400	1.3	1.4	4.1	4.4
500	22	23	31	35
600	148	152	(118)	140
700	554	582	–	378
800	1514	1590	–	793
900	3312	3474	–	(1411)
1000	(6194)	(6494)	–	(2239)

The Gibbs free energy of Na_2O in equilibrium with Na(O) was quoted by Fredrickson and Chasanov as ${}^f\Delta G°<Na_2O>$ = - 421700 + 146.4·T J/mol [4], the probably congruent melting point of Na_2O is T_m = 1407 K (1134 °C). The relative partial molar Gibbs energy and the partial pressure of oxygen in the Na-O system was calculated as a function of the oxygen concentration c_O ($c_O \leq c_O°$) by Sieverts' law using the data of Fredrickson and Chasanov [4] and of Noden [2], c_O in wt.-ppm: $\Delta\overline{G}_{O_2} = RT \ln p_{O_2}$ = - 749800 + 53.2·T + 38.3·T·log c_O J/mol O_2. This correlation is graphically presented for different c_O in fig. 4. Replacement of Noden's data by that of Thorley gives $\Delta\overline{G}_{O_2} = RT \ln p_{O_2}$ = - 774000 + 96·T + 39.1·T·log c_O J/mol O_2.

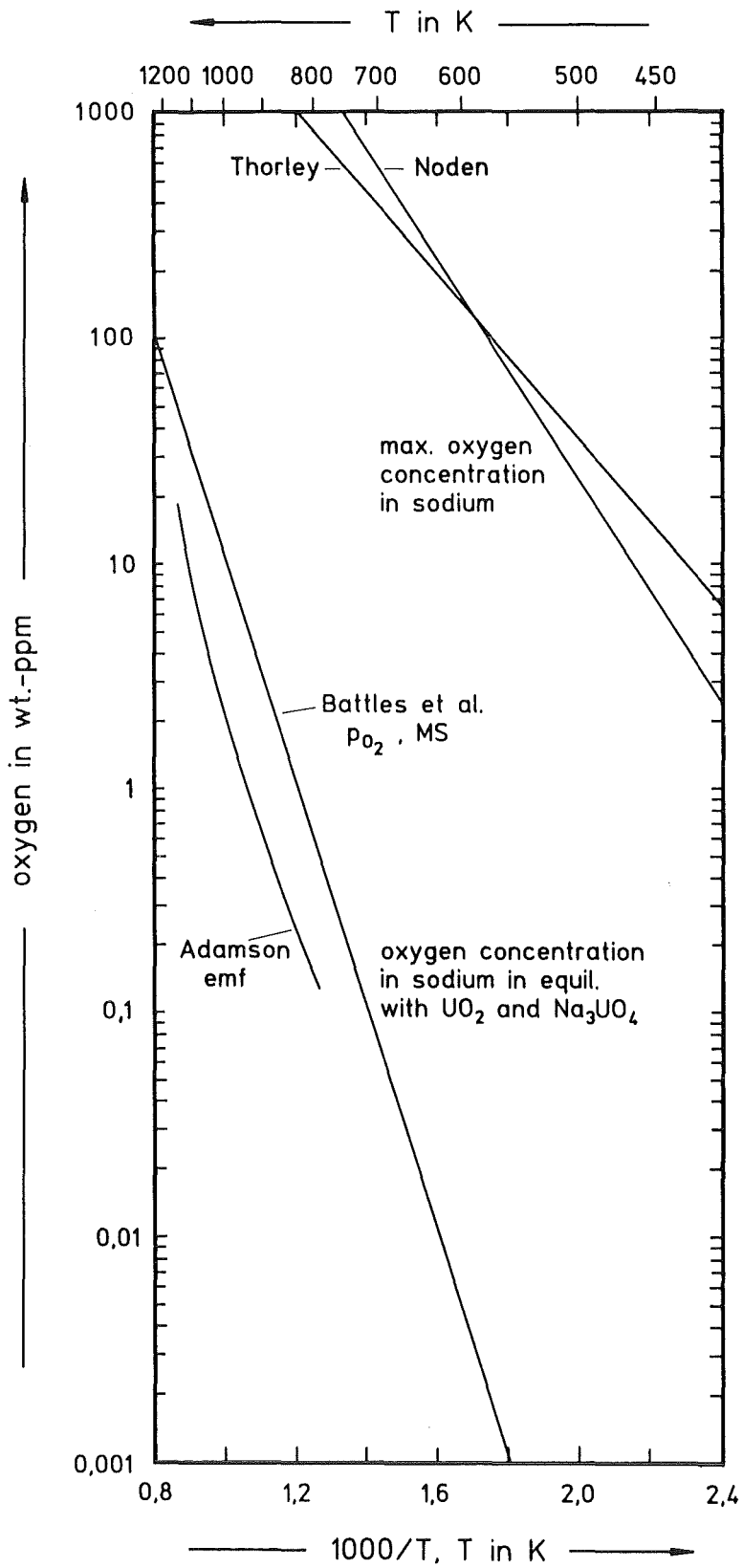

Fig. 3: Maximum oxygen concentration in sodium and oxygen concentration in sodium in equilibrium with UO_2 and Na_3UO_4.

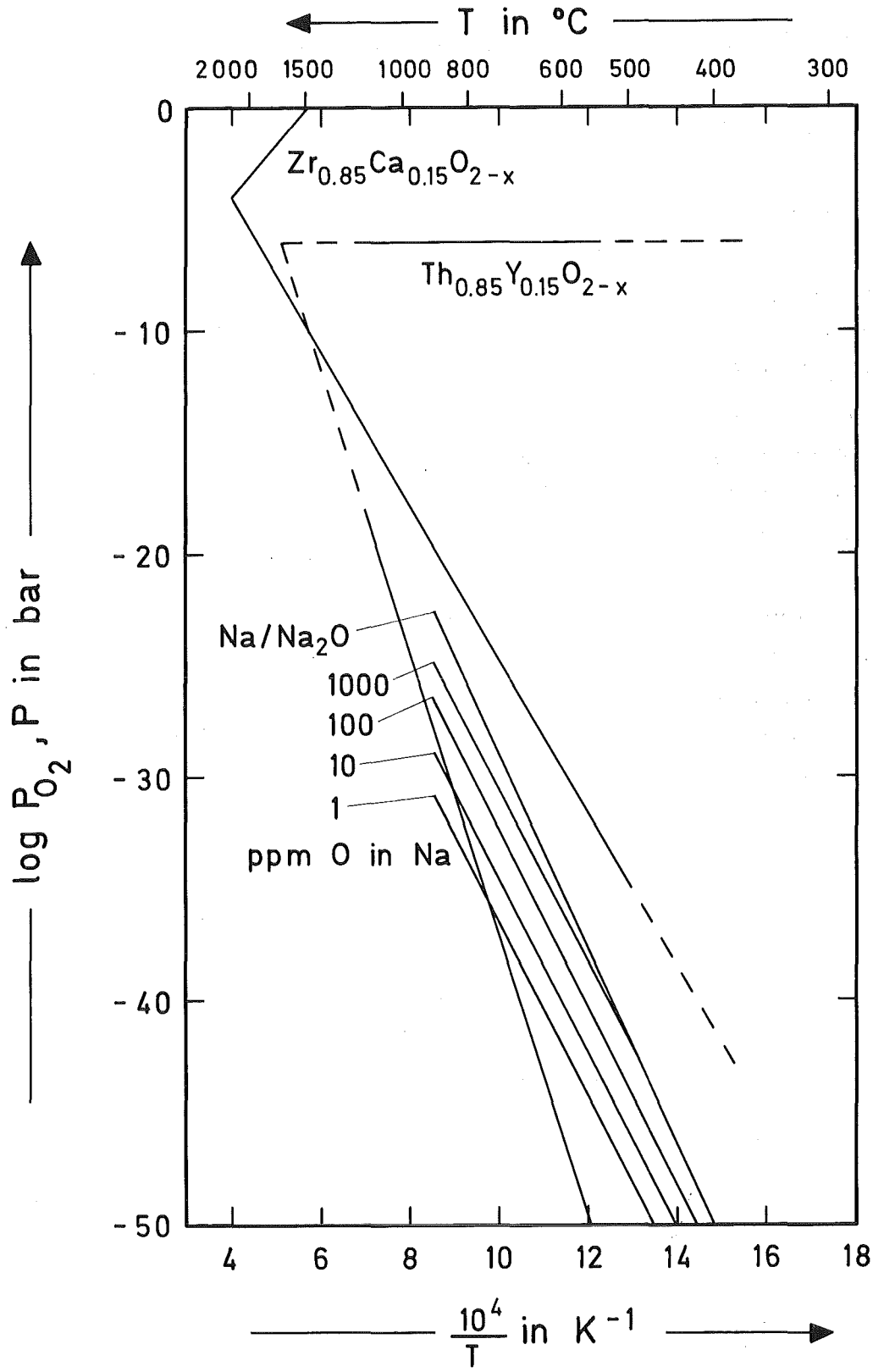

Fig. 4: Oxygen partial pressures of Na(O) solutions for given oxygen concentrations in wt.-ppm. The p_{O_2}-T field is added where oxygen partial pressure measurements by the emf method are possible with ZrO_2 and ThO_2 electrolytes.

3. The Na-U-O, Na-Pu-O and Na-U-Pu-O systems

3.1 The phase diagrams

Na-U-O system

A series of sodium uranates are described in the Na-U-O system: Na_3UO_4 with a narrow homogeneity range $Na_{3-x}U_{1+x}O_4$ up to x = 0.1 at 1000 K and probably a homogeneity range up to the composition Na_4UO_4 at low temperatures [44], Na_4UO_5, Na_2UO_4, $NaUO_3$, $Na_2U_2O_7$, $Na_6U_7O_{24}$, $Na_2U_{13}O_{40}$ and possibly a phase of the composition $Na_{5.3}UO_5$ [44]. Tentative isothermal sections of the Na-U-O system were published in [5,6]. An isothermal section at about 1000 K (about 700 °C) is presented in fig. 5. The coexistence of Na(O), UO_2 and Na_3UO_4 was proven [5,7]. Hence, stoichiometric UO_2 does not react with pure sodium.

The compound Na_3UO_4 is of particular interest because $Na_3(U,Pu)O_4$ is formed during the reaction of sodium with $(U,Pu)O_2$. The physical properties of the isotypic compounds $Na_3U_{1-x}Pu_xO_4$ ($x \leq 0.3$) and Na_3UO_4 are believed to be similar. Na_3UO_4 was first synthezised by Scholder and Gläser [8]. The relative molecular mass is 371.0.

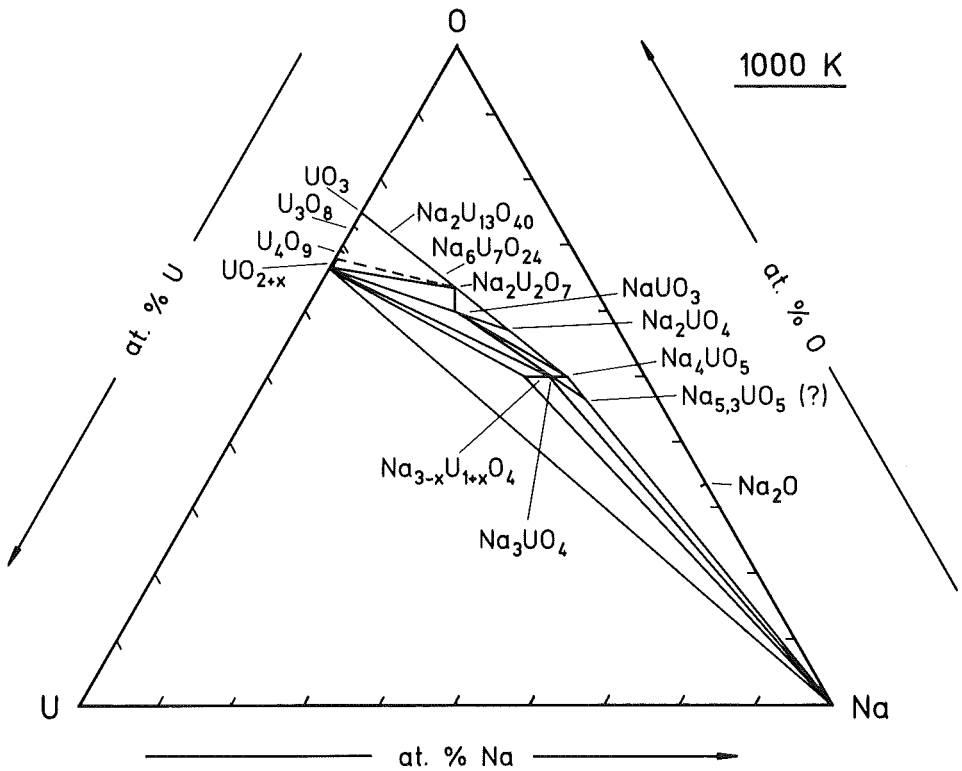

Fig. 5: Isothermal section of the ternary Na-U-O system at 1000 K.

Na-Pu-O system

The following sodium plutonates were observed in the Na-Pu-O system: Na_3PuO_4, Na_4PuO_5, Na_6PuO_6 [38,39], Na_2PuO_3, $Na_4Pu_2O_5$, Na_4PuO_4 and Na_6PuO_5 [44]. Na_3PuO_4 is not isotypic with Na_3UO_4, hence there is no complete miscibility. Na_3PuO_4 and Na_2PuO_3 form a complete series of solid solutions. Na_3PuO_4 does not coexist with sodium. Coexisting phases are Na(O), $PuO_{1.6}$ and $Na_4Pu_2O_5$. A tentative isothermal section of the Na-Pu-O system at about 1000 K (about 700 °C) based on the present knowledge is illustrated in fig. 6.

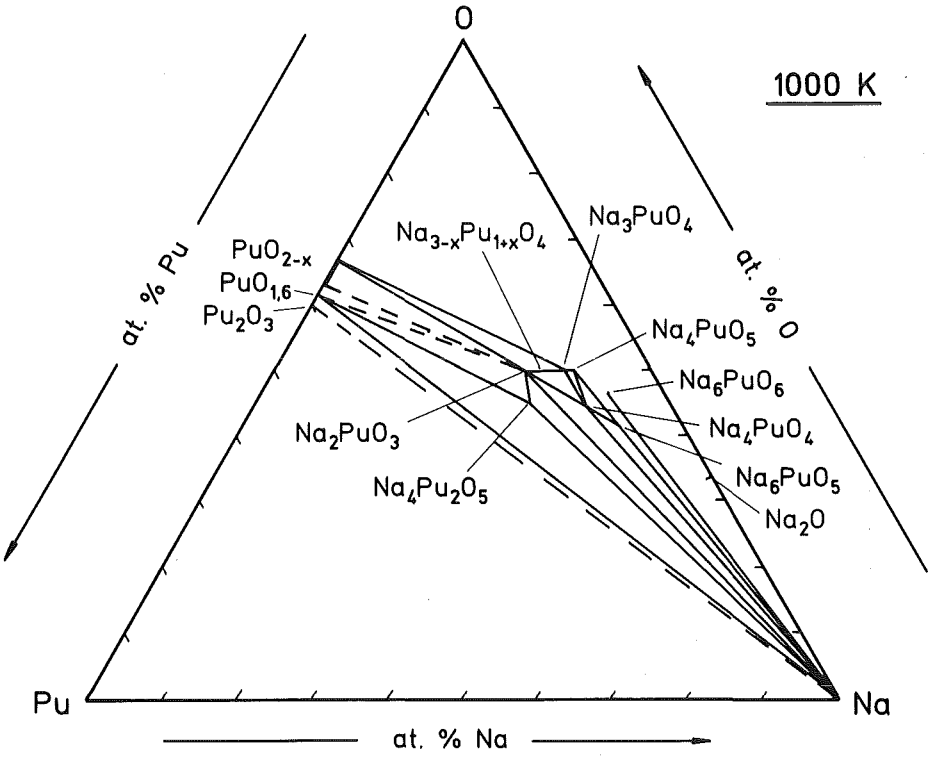

Fig. 6: Tentative isothermal section of the ternary Na-Pu-O system at 1000 K.

Na-U-Pu-O system

As the thermodynamically stable phases Na_3UO_4 and Na_3PuO_4 are not completely miscible, a two-phase region must occur in the pseudobinary Na_3UO_4-Na_3PuO_4 section of the quaternary Na-U-Pu-O system. The relevant state space is sketched in [46]. $Na_3(U,Pu)O_4$ has a homogeneity range in both the directions of $Na_2(U,Pu)O_3$ and $Na_4(U,Pu)O_5$ [44]. Metastable $Na_3U_{0.72}Pu_{0.28}O_4$ is isotypic with rhombohedral Na_3PuO_4. The U/Pu ratios of the sodium uranoplutonates observed in the pseudoternary Na-$U_{0.72}Pu_{0.28}$-O system are the same as that of the oxide [29,44].

3.2 Crystallographic properties

Na-U-O system

The crystallographic data and X-ray densities of the sodium uranates were taken from Landolt-Börnstein [9] with the exception of α- and β-Na_3UO_4 [44] and are compiled in table 2.

Table 2: Crystallographic data and X-ray densities of sodium uranates.

phase	system	type	lattice parameters in pm			ρ_x in Mg/m^3
			a	b	c	
m-Na_3UO_4	cubic	NaCl	477	–	–	5.68
β-Na_3UO_4[a]	cubic (h)	NaCl s.l.	959	–	–	5.59
α-Na_3UO_4[b]	tetrag. (l)		951.2	–	967.6	5.63
$NaUO_3$	o'rh.	$GdFeO_3$	577.6	591.0	828.3	7.26
β-Na_4UO_5	tetr. (h)	Li_4UO_5	757.6	–	464.1	5.11
α-Na_4UO_5	cubic (l)	NaCl	476.6	–	–	5.03
β-Na_2UO_4	o'rh. (h)	Na_2UO_4 (I)	597.9	580.7	1172.4	5.68
α-Na_2UO_4	o'rh. (l)	Na_2UO_4 (II)	976.9	573.4	349.8	5.90
$Na_2U_2O_7$	monocl.	$CaUO_4$ s.l.	1279.6	782.2	689.6	6.6
			β =	111.42°		
$Na_6U_7O_{24}$	triclinic					
$Na_2U_{13}O_{40}$	o'rh.		680.7	1593.4	825.4	7.2

s.l.: super lattice structure. [a]T > 1000 °C, [b]T < 1000 °C.

Na_3UO_4 is the most important compound in the Na-U-O system which crystallizes in a distorted cubic form with the lattice parameter a = 478 - 480 pm, space group Fm3m, Z = 1 [10]. This form is believed to be a metastable one (m-Na_3UO_4) existing below 600 °C [44]. The lattice parameter of this metastable Na_3UO_4 was further reported: a = 477 pm, formulated as $[Na_{0.75}U_{0.25}]^{++}[O]^{--}$, cations statistically distributed [8], a = 479 - 480 pm [7], a = 478 - 479 pm [6], a = 480 pm [11]. The stable Na_3UO_4 exists obviously in two modifications with a transition

point at about 1000 °C, the high temperature β-Na_3UO_4 being fcc., the low temperature α-Na_3UO_4 being tetragonal [44]. The reflexes of the presumed β-Na_3UO_4 could be indexed only by doubling of the elementary cell to a = 954.4 pm; this cell contains 32 metal and 32 oxygen atoms; the space group is Fd3m [10]. Na_3UO_4 was further indexed by assuming a primitive cubic cell with 2·477 = 954 pm, the space group is $P4_232$ and the composition $Na_{11}U_5O_{16}$ [12]. The existence of a phase $Na_{11}U_5O_{16}$ was suggested in [13] and was denied in [44]. A Na_3UO_4 - $Na_{3-x}U_{1+x}O_4$ solid solution ($x \leq 0.25$, x = 0.1 at 1000 K) was observed [44]. However, this sodium uranate solid solution would be the only one with a uranium valency less than five; the mean valency would decrease down to 4.2. $Na_2U_2O_7$ was also indexed by a pseudohexagonal cell (space group R3m): a ≈ 395 pm, c ≈ 1782 pm [9]. The structure of $NaUO_3$ (space group Pbnm) was first determined in [26]: a = 577.5 pm, b = 590.5 pm, c = 825.0 pm, ρ_x = 7.30 Mg/m^3. A most recent determination of the lattice parameters of this phase is reported in [50]. According to [44], Na_4UO_5 exists only in one crystallographic form, the tetragonal form: a = 754.6 pm, c = 463.7 pm.

Na-Pu-O system

The crystallographic data of the sodium plutonates were taken from Keller et al. [38,39] and from the thesis of Pillon [44]. The X-ray densities were calculated and added by the present author. The data are compiled in table 3. A NaCl-type superlattice structure of Na_3PuO_4 was suggested in [40]. The reported lattice parameter of this phase is a = 488 pm [21] and a = 486 pm [41,46] resp. and could be attributed to the composition $Na_4Pu_2O_5$ found by Pillon [44].

Na-U-Pu-O system

Different structures and lattice parameters were observed for the metastable and for the thermodynamically stable sodium uranoplutonates $Na_3(U,Pu)O_4$ which are compiled in table 4. Crystallographic data of further sodium uranoplutonates are reported in [44]: $Na_2U_{0.72}Pu_{0.28}O_3$, a = 479.5 pm, and $Na_{3.5}U_{0.72}Pu_{0.28}O_{4.5}$, a = 477.6 pm which are both miscible with $Na_3U_{0.72}Pu_{0.28}O_4$; $Na_4U_{0.72}Pu_{0.28}O_4$, a = 479.0 pm.

Table 3: Crystallographic data and X-ray densities of sodium plutonates.

phase	system	type	lattice parameters			ρ_x in Mg/m³
			a in pm	c in pm	α in °	
Na_3PuO_4	rhomboh.		678.1	–	60.67	5.52
γ-Na_4PuO_4[a]	cubic		479.7	–	–	5.94
β-Na_4PuO_4[b]	rhomboh.		679.5	–	60.73	5.82
α-Na_4PuO_4[c]	cubic		479.0	–	–	5.97
Na_2PuO_3	rhomboh.		681.1	–	60.67	
$Na_4Pu_2O_5$	cubic		488.0	–	–	
Na_4PuO_5	tetrag.		751.5	461.9	–	5.23
β-Na_4PuO_5	tetrag. (h)	Li_4UO_5	744.9	459.0	–	5.36
α-Na_4PuO_5	cubic (l)	NaCl	471.8	–	–	5.20
Na_6PuO_6	hexag.	Li_6ReO_6 (II)	576	1590	–	5.16

[a]T > 900 °C; [b]650 - 900 °C; [c]T < 650 °C

Table 4: Observed lattice parameters of $Na_3(U,Pu)O_4$.

composition	reaction temperature	structure	lattice parameters			Ref.
			a in pm	c in pm	α in °	
$Na_3U_{0.7}Pu_{0.3}O_4$	600-900 °C	tetrag.	477	488	–	21
$Na_3U_{0.24}Pu_{0.76}O_4$	600-900 °C	tetrag.	479	492.5	–	21
$Na_3U_{0.7}Pu_{0.3}O_4$	850 °C	tetrag.	478	488	–	46
$Na_3U_{0.7}Pu_{0.3}O_4$	550 °C	cubic	480	–	–	46
$Na_3U_{0.72}Pu_{0.28}O_4$	600-1000 °C	cubic	479.5	–	–	44
m-$Na_3U_{0.72}Pu_{0.28}O_4$[a]	600-1000 °C	rhomboh.	675.7	–	60.4	44
$Na_{3+x}U_{0.72}Pu_{0.28}O_4$	≤ 1000 °C	cubic	479			44

[a]metastable

3.3 Mechanical properties

Hardness

The room temperature Vickers hardness HV of Na_3UO_4 with 97 % th.d. and < 10 vol.% of second phases ($NaUO_3$ and UO_2) was reported to 480 - 600 HV under 1 N load; the most probable value is (500 ± 100) HV [14].

Elastic constants

The isothermal and the adiabatic Young's modulus E of Na_3UO_4 with 97 % th.d. were measured at room temperature by compression experiments and by longitudinal velocity of sound measurements (c_L = 3550 m/s),resp. This results in E_{is} = (70 ± 5) GN/m^2 for the isothermal Young's modulus. The adiabatic Young's modulus was evaluated by application of the expression $E_{ad} = c_L^2 \cdot \rho\ (1 + \mu)(1 - 2\mu)/(1 - \mu)$ with ρ = 5.45 Mg/m^3 and an estimated Poisson's number μ = 0.25 yielding E_{ad} = 58 GN/m^2 [14]. The weighed averaged is E = (60 ± 3) GN/m^2 [49]. This would lead to G = 24 GN/m^2 for the shear modulus and B = 40 GN/m^2 for the bulk modulus. The adiabatic Young's modulus was further determined on Na_3UO_4 with 93 - 95 % th.d. by the same method of velocity of sound (c_L = 5630 m/s). Using ρ = 5.42 and an estimated μ = 0.3, the adiabatic Young's modulus gives E_{ad} = 128 GN/m^2 at room temperature [20]. The reasons for the discrepancy of the results of the two authors are not known at the moment.

Compressive rupture strength

The room temperature compressive rupture strength of Na_3UO_4 with 97 % th.d. is higher than 230 MN/m^2 [14]. Further measurements on Na_3UO_4 with 93 - 95 % th.d. give 132 MN/m^2 [20]. The different results of the two authors cannot be explained alone by the different densities; the reasons are not known at the moment.

Creep

Creep experiments under compression (σ = 10 - 20 MN/m^2) were performed on Na_3UO_4 pellets with 87 % th.d. between 700 and 900 °C up to 200 hours. The creep law between 750 and 900 °C can be described by the relation $\dot{\varepsilon} \sim \sigma^n \cdot \exp(-Q/RT)$ with the stress exponent n = 1.5 and the activation energy Q = (250 ± 20) kJ/mol [37]. The creep mechanism obeys another law below 750 °C. The creep rate $\dot{\varepsilon}$ is presented for two compressive stresses σ = 10 and 20 MN/m^2 in fig. 7.

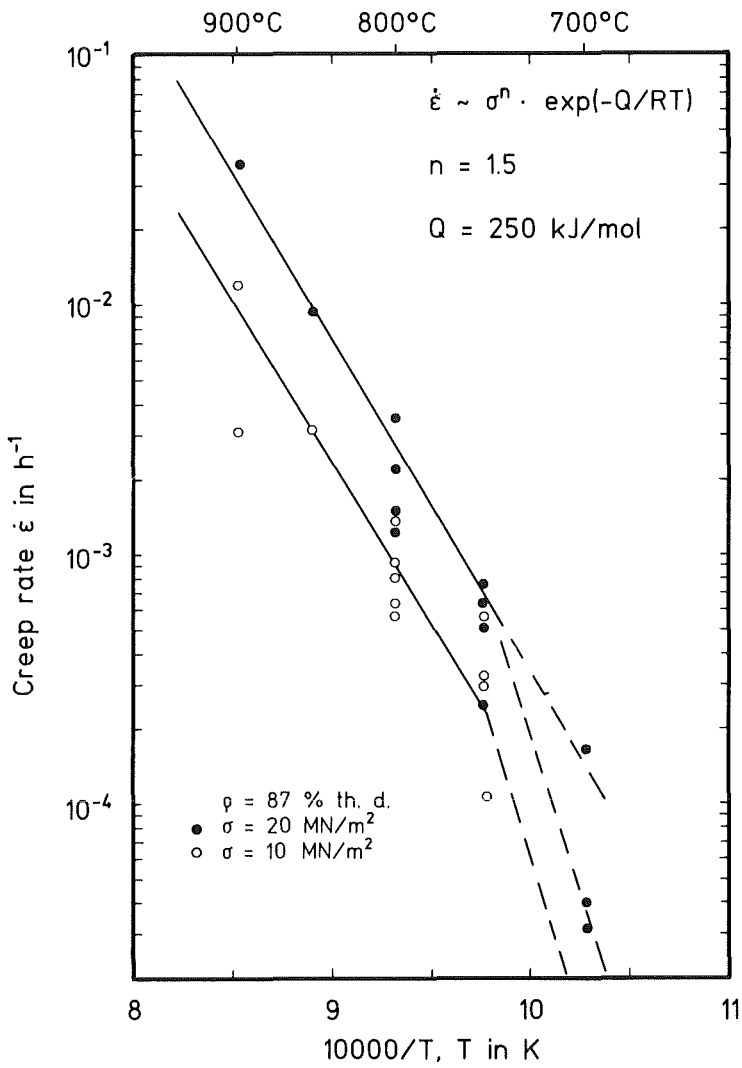

Fig. 7: Compressive creep of Na_3UO_4 [37].

3.4 Thermal and thermodynamic properties

Thermal expansion

The linear thermal expansion $\Delta l/l_0$ of $Na_3UO_{4.08}$ with 90 % th.d. and < 8 vol.% second phases was measured by dilatometry between room temperature and 800 °C with 6 K/min heating rate under unknown atomspheric conditions [15]. The linear thermal expansion is 1.3 % at 800 °C, see fig. 8. An irregular behaviour was observed below 300 °C. The linear back extrapolation to room temperature gives a linear thermal expansion coefficient $\alpha_{20} = 13 \cdot 10^{-6}\ K^{-1}$ at 20 °C, see fig. 9. The linear thermal expansion $\Delta l/l_0$ was further measured on Na_3UO_4 with 93 % th.d. and < 10 vol.% second phases ($NaUO_3$ and UO_2) by dilatometry between 100 and 900 °C [19]; $\Delta l/l_0 = -4 \cdot 10^{-4} + 20 \cdot 10^{-6} \cdot T + 3 \cdot 10^{-9} \cdot T^2$ and $\Delta l/l_0$ = 1.75 % at 800 °C, see fig. 8. The linear thermal expansion coefficient gives

$\alpha = 20 \cdot 10^{-6} + 6 \cdot 10^{-9} \cdot T\ K^{-1}$ between room temperature and 900 °C; at 20 °C, $\alpha_{20} = 20 \cdot 10^{-6}\ K^{-1}$, see fig. 9. The discrepancy of the two data sets of the linear thermal expansion cannot be explained at the moment. Further mean linear thermal expansion coefficients $\bar{\alpha}$ measured by high temperature lattice parameters are reported in [44]: Na_3UO_4: $\bar{\alpha} = 28 \cdot 10^{-6}\ K^{-1}$ (0 - 1000 °C); Na_4UO_4: $\bar{\alpha} = 24 \cdot 10^{-6}\ K^{-1}$ (0 - 500 °C); $Na_{5.3}UO_5$: $\bar{\alpha} = 28 \cdot 10^{-6}\ K^{-1}$ (0 - 1000 °C).

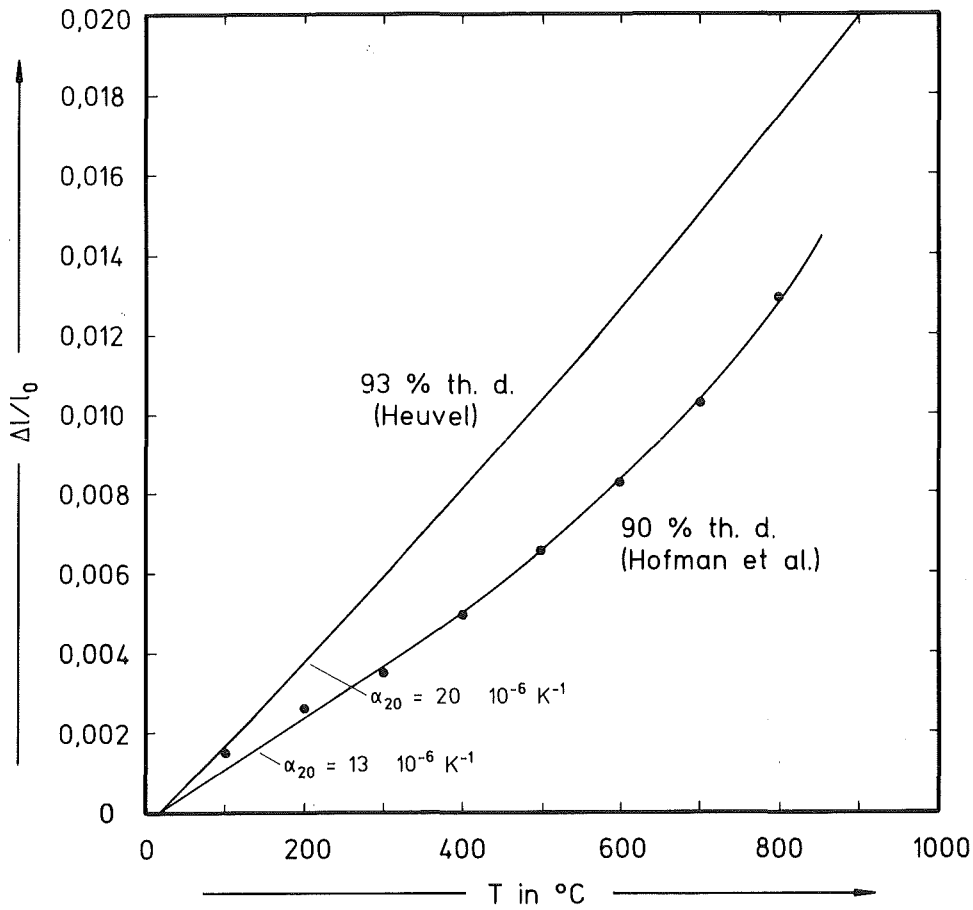

Fig. 8: Linear thermal expansion $\Delta l/l_0$ of Na_3UO_4 .

Heat capacity, thermodynamic properties

The heat capacity of Na_3UO_4 was measured with an adiabatic calorimeter at low temperatures between 5 and 350 K. The heat capacity at 298 K is $C_{p,298} = (173.0 \pm 0.4)$ J/K·mol, the standard entropy at 298 K is $S°_{298} = (198.2 \pm 0.4)$ J/K·mol, the enthalpy at 298 K is $H°_{298} - H°_0 = (31109 \pm 62)$ J/mol [16]. The heat capacity was determined at high temperatures between 500 and 1200 K with a drop calorimeter. The enthalpy is $H°_T - H°_{298} = 188.9009 \cdot T + 0.01258940 \cdot T^2 + 2080067 \cdot T^{-1} - 64416.49$ (J/mol). The heat capacity is $C_{p,T} = 188.9009 + 0.0251788 \cdot T - 2080067 \cdot T^{-2}$ (J/K·mol) [17], see fig. 10. Differing results of the heat capacity of Na_3UO_4 between room temperature and 900 °C were published in

[15]; they are disregarded. Further, the heat capacities of Na_3UO_4, Na_3PuO_4 ($C_{p,298}$ = 165 J/K·mol) and $Na_3U_{0.72}Pu_{0.28}O_4$ were graphically represented between 300 and 1050 K in [44]. The enthalpy, heat capacity, entropy and Gibbs free energy of formation of Na_3UO_4 between 298 and 1200 K are compiled in table 5. The heat of formation of Na_3UO_4 was measured as ${}^f\Delta H°_{298}$ = - (1998.7 ± 3.8) kJ/mol [27]. This value was later revised by [45,48] and is recommended by ${}^f\Delta H°_{298}$ = - (2022 ± 3) kJ/mol. A least-squares fit of the revised numerical data of the Gibbs free energy of formation of Na_3UO_4 is given by ${}^f\Delta G°$ = - 2027 + 0.432·T kJ/mol, 298 - 1200 K. The available thermodynamic data of the sodium uranates at room temperature are summarized in table 6. A complete set of numerical data of these thermodynamic properties is assessed in [48].

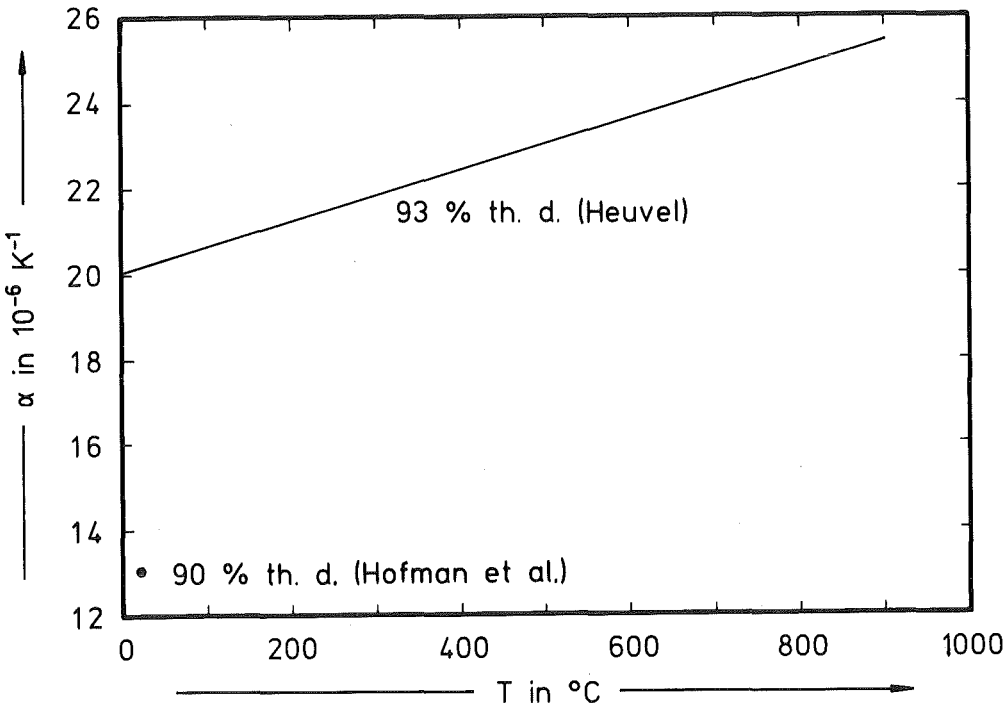

Fig. 9: Linear thermal expansion coefficient α of Na_3UO_4.

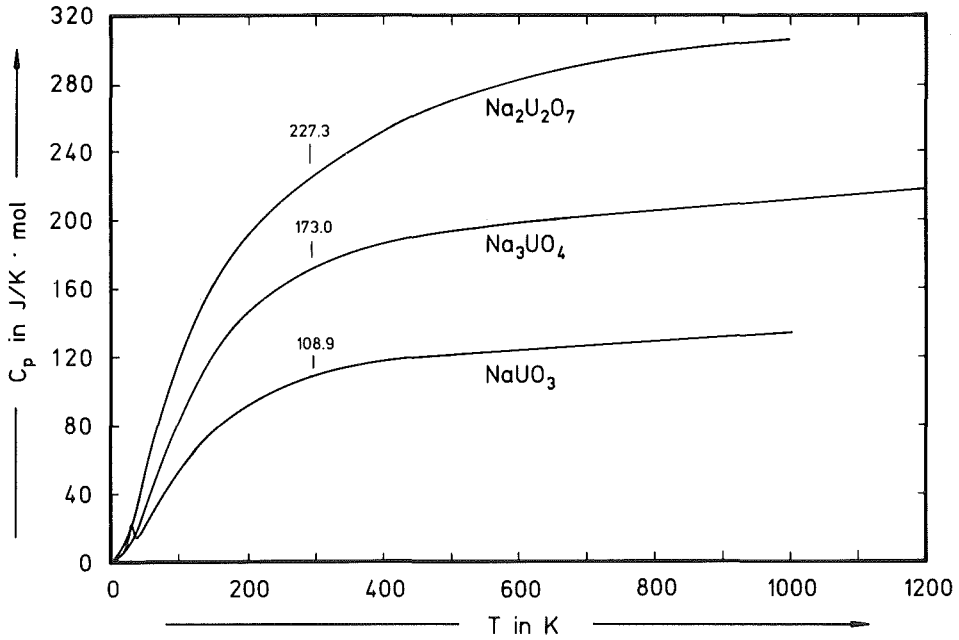

Fig. 10: Heat capacity C_p of $Na_2U_2O_7$, Na_3UO_4 and $NaUO_3$ [16,17].

Table 5: Enthalpy $H^\circ_T - H^\circ_{298}$, heat capacity $C_{p,T}$, standard entropy S°_T and Gibbs free energy of formation ${}^f\Delta G^\circ_T$ of Na_3UO_4 [16,17].

T in K	$H^\circ_T - H^\circ_{298}$ in J/mol	$C_{p,T}$ in J/K·mol	S°_T in J/K·mol	${}^f\Delta G^\circ_T$ in kJ/mol*
298	0	173.0	198.2	- 1898
400	18359	186.0	251.1	- 1855
500	37341	193.2	293.4	- 1812
600	56923	198.2	329.1	- 1768
700	76955	202.3	359.9	- 1725
800	97362	205.8	387.2	- 1682
900	118103	209.0	411.6	- 1638
1000	139154	212.0	433.8	- 1595
1100	160499	214.9	454.1	- 1552
1200	182127	217.7	473.0	- 1501

*revised [45,48]: ${}^f\Delta G^\circ = -2027 + 0.432 \cdot T$ kJ/mol, 298 - 1200 K.

Table 6: Thermodynamic data of sodium uranates at 298 K; for temperature functions T ≥ 298 K see references.

compound	$H°_{298} - H°_0$ in J/mol	$C_{p,298}$ in J/K·mol	$S°_{298}$ in J/K·mol
Na_3UO_4	31109 ± 62 [16]	173.0 ± 0.4 [16]	198.2 ± 0.4 [16]
$NaUO_3$	20176 ± 20 [34]	108.9 ± 0.1 [34]	132.8 ± 0.1 [34]
α-Na_2UO_4	26277 ± 52 [31]	146.7 ± 0.3 [31]	166.0 ± 0.3 [31]
α-$Na_2U_2O_7$	41868 ± 126 [35]	227.3 ± 0.7 [35]	275.9 ± 0.8 [35]

compound	$^f\Delta H°_{298}$ in kJ/mol	$^f\Delta G°_{298}$ in kJ/mol
Na_3UO_4	- 1998.7 ± 3.8 [27]	- 1874 ± 4 [16]
	- 2022 ± 2.5 [45]*	- 1898 ± 3 [45]*
$NaUO_3$	- 1495.8 ± 3.3 [32]	- 1413 ± 3 [34]
α-Na_2UO_4	- 1864.2 ± 3.6 [30]	- 1746 ± 4 [31]
	- 1897.3 ± 1.1 [35]	
β-Na_2UO_4	- 1850.4 ± 3.6 [33]	
α-$Na_2U_2O_7$	- 3194.8 ± 1.8 [35]	- 3002 [35]
Na_4UO_5	- 2450.6 ± 2.1 [48]	

* recommended values

Vapour pressure

Vapour pressure measurements in the Na-U-O system are reported by Battles et al. [28]. The partial pressures were determined in the three-phase fields by mass-spectrometry between 600 and 1400 K. In the most important phase field Na-UO_2-Na_3UO_4, only the gaseous species Na was observed below 1175 K. Above 1275 K, Na and O_2 were detected. Na_3UO_4 dissociates in this temperature range by evaporation. The condensed phase is enriched in sodium poorer uranates. The oxygen partial pressure according to the reaction $<Na_3UO_4> = 3\ \{Na\} + <UO_2> + (O_2)$ could not be directly measured due to the low oxygen pressure and was calculated by use of the experimental data of the neighbouring phase fields. The relative partial molar Gibbs energy of oxygen in the Na-UO_2-Na_3UO_4 three-phase field is $\Delta\bar{G}_{O_2} = RT \ln p_{O_2} = -922600 + 262 \cdot T$ J/mol O_2 between 600 and 1200 K [28]. A second set of data was evaluated by Adamson et al. from calorimetric measurements resulting in $\Delta\bar{G}_{O_2} = RT \ln p_{O_2} = -945000 + 261 \cdot T$ J/mol O_2 between 700 and 1200 K [29]. A third set of data is based on direct EMF cell studies reported in [29] and by Mignanelli and Potter [41]; the latter quote $\Delta\bar{G}_{O_2} = RT \ln p_{O_2} = -949800 + 253 \cdot T$ J/mol O_2 between 800 and 1000 K. The numerical values are compared in table 7. The latter two sets [29,41] should be preferred.

Table 7: Oxygen partial pressure p_{O_2} and relative partial molar Gibbs free energy of oxygen $\Delta\bar{G}_{O_2}$ of Na_3UO_4 in equilibrium with Na and UO_2.

T in K	log p_{O_2} in bar			$\Delta\bar{G}_{O_2}$ in kJ/mol O_2		
	Battles [28]	Adamson [29]	Mignan. [41]	Battles [28]	Adamson [29]	Mignan. [41]
600	- 66.7	(- 68.6)	(- 69.5)	- 766	(- 788)	(- 798)
700	- 55.2	- 56.9	(- 57.7)	- 740	- 762	(- 773)
800	- 46.6	- 48.1	- 48.8	- 713	- 736	- 747
900	- 39.9	- 41.2	- 41.9	- 687	- 710	- 722
1000	- 34.5	- 35.7	- 36.4	- 661	- 684	- 697
1100	- 30.1	- 31.2	(- 31.9)	- 635	- 657	(- 671)
1200	- 26.5	- 27.5	(- 28.1)	- 609	- 631	(- 646)

The oxygen and sodium partial pressures in the three-phase fields of the Na-U-O system were calculated as a function of temperature from the mass-spectrometric measurements [28], they are given at 1000 K in table 8.

Table 8: Oxygen and sodium partial pressures in the three-phase fields of the Na-U-O system at 1000 K [28].

phases	p_{O_2} in bar	p_{Na} in bar
UO_2-Na-Na_3UO_4	$3.2 \cdot 10^{-35}$	0.17
UO_2-$NaUO_3$-Na_3UO_4	$9.6 \cdot 10^{-19}$	$5.5 \cdot 10^{-7}$
$NaUO_3$-Na_3UO_4-Na_4UO_5	$5.0 \cdot 10^{-16}$	$1.2 \cdot 10^{-7}$
$NaUO_3$-Na_2UO_4-Na_4UO_5	$5.3 \cdot 10^{-15}$	$5.3 \cdot 10^{-8}$
$NaUO_3$-Na_2UO_4-$Na_2U_2O_7$	$1.6 \cdot 10^{-11}$	$9.6 \cdot 10^{-10}$

The oxygen concentration in sodium in equilibrium with $U_{0.8}Pu_{0.2}O_{2-x}$ and $Na_3(U,Pu)O_4$ and the limiting O/(U + Pu) ratio of the mixed oxide fuel were calculated with the maximum oxygen solubility in sodium, the Gibbs free energy of formation of Na_2O and the oxygen partial pressure measurements in the Na-U-O system and in the $(U,Pu)O_{2-x}$ system [28]. The data is compiled in table 9. However, many other and contradictory results of the limiting O/(U + Pu) ratio of the mixed oxide fuel are available. Four sets of oxygen concentrations in sodium in equilibrium with UO_2 and Na_3UO_4 were evaluated using the relative partial molar Gibbs energy of oxygen in the three-phase field by Battles et al. [28], Adamson et al. [29] and Mignanelli and Potter [41], resp., in table 7 and using the maximum oxygen concentration in sodium by Noden [2] and Thorley [3,47], resp., in table 1. The results are also compiled in table 9, two are illustrated in fig. 3. The second and third sets in table 9 should be preferred, however, the differing results are subject for further discussions.

Thermal stability

The dissociation temperature of Na_3UO_4 was measured by DTA/TGA under flowing helium gas at 1 K/min heating rate. The dissociation begins at 1050 °C. Na_3UO_4 decomposes probably into $NaUO_3$ and UO_2 [19]. Heating of Na_3UO_4 under vacuum (10^{-5} bar) at 900 °C for three hours results in solid $NaUO_3$ and gaseous Na_2O which volatilizes [8]. Based on the findings of [28] the decomposition of Na_3UO_4 under vacuum should take place according to the reaction $<Na_3UO_4>$

Table 9: Oxygen distribution in the Na(O)-$U_{0.8}Pu_{0.2}O_{2-x}$-$Na_3(U,Pu)O_4$ three-phase field of the pseudoternary Na-U, Pu-O system after Battles et al. [28] and in the Na(O)-UO_2-Na_3UO_4 three-phase field of the ternary Na-U-O system using the equilibrium oxygen potential of Battles et al. [28], Adamson et al. [29] and Mignanelli [41], resp., and the maximum oxygen solubility in sodium of Noden [2] and Thorley [3,47], resp., and Sievert's law.

T in K	Na(O)-$U_{0.8}Pu_{0.2}O_{2-x}$-$Na_3(U,Pu)O_4$		Na(O)-UO_2-Na_3UO_4			
	O/(U + Pu) in the fuel	$\lvert O \rvert_{Na}$ in wt.-ppm in sodium	$\lvert O \rvert_{Na}$ in wt.-ppm in sodium			
			B. + N.	A. + N.	M. + N.	M. + T.
600	1.92	0.005	0.008	0.001	–	–
700	1.93	0.08	0.10	0.014	0.005	0.004
800	1.94	0.6	0.63	0.12	0.044	0.022
900	1.945	3.1	2.7	0.6	0.23	0.094
1000	1.95	11	8.5	2.1	0.88	0.30
1100	1.956	32	22	6.5	2.6	0.76
1200	1.96	77	48	15	6.5	1.6

= <$NaUO_3$> + 2(Na) + 1/2 (O_2). α-Na_2UO_4 decomposes above 750 °C [11]. Na_4UO_5 decomposes in air at about 1000 °C [11]. $Na_2U_2O_7$ is stable in air up to 1300 °C [11].

Na_3PuO_4 decomposes into PuO_2 and volatile sodium oxides at 1000 °C [38,39]. Na_2PuO_3 is stable up to 1200 °C [44].

3.5 Transport properties

Thermal diffusivity and thermal conductivity

The thermal diffusivity α of Na_3UO_4 with < 10 vol.% second phases and densities between 80 and 96 % th.d. was measured between room temperature and 600 °C by the laser flash technique. The results are illustrated in fig. 11; $\alpha = 5.3 \cdot 10^{-7}$ m^2/s at 20 °C and about 92 % th.d. [18]. The thermal diffusivity and the thermal conductivity $\lambda = c \cdot \rho \cdot \alpha$ were corrected to 100 % th.d. considering open and closed porosity, pore form and pore orientation which results in a thermal

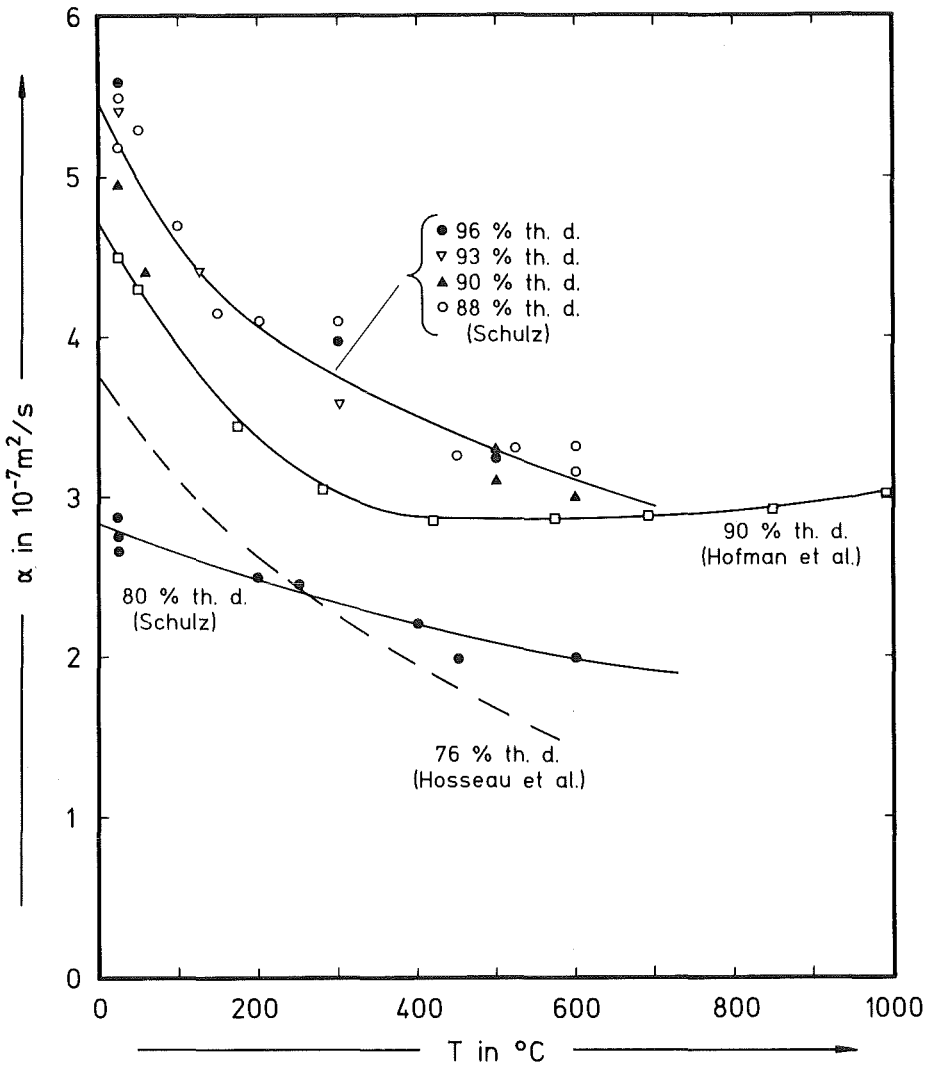

Fig. 11: Thermal diffusivity α of Na_3UO_4 with different densities.

diffusivity value $\alpha_0 = 5.8 \cdot 10^{-7}$ m²/s at 20 °C. The thermal conductivity of Na_3UO_4 with 100 % th.d. was calculated using the heat capacity data of [17] which gives $\lambda_0 = 100/(74.6 + 0.052 \cdot T)$ W/m·K between room temperature and 600 °C and $\lambda_0 = 1.32$ W/m·K at 20 °C, see fig. 12. The thermal diffusivity α was further measured on Na_3UO_4 with < 8 vol.% second phases and 90 % th.d. by the laser flash technique up to 1000 °C [15], see fig. 11. The thermal conductivity λ was corrected to 100 % th.d. by the relation $\lambda_0 = \lambda\,(1 + 0.5 \cdot P)/(1 - P)$ and with the author's [15] heat capacity data which differ from those of [17]. The thermal conductivity at 20 °C is $\lambda_0 = 1.48$ W/m·K. The results are presented in fig. 12; they are higher than those of [18] due to the use of the obviously incorrect heat capacity data at high temperatures given in [15].

Older results of the thermal diffusivity of Na_3UO_4 with 76 % th.d. between room temperature and 500 °C are reported in [21], see fig. 11. The thermal conductivity originally calculated with an estimated heat capacity was recalculated with the

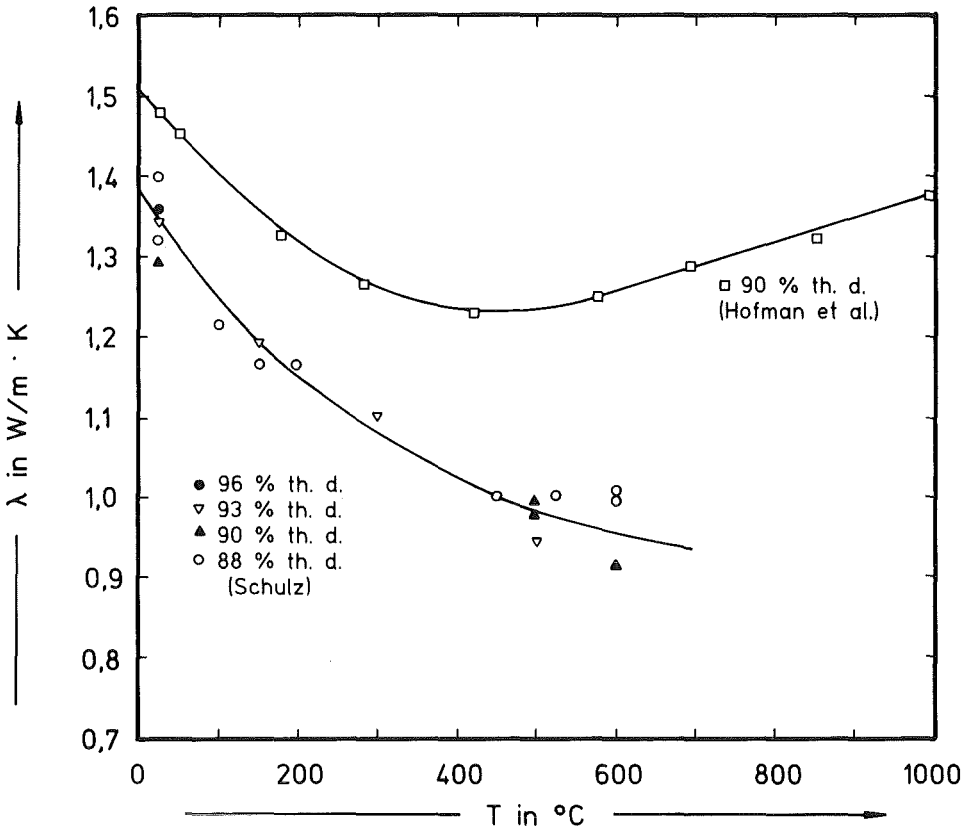

Fig. 12: Thermal conductivity λ of Na_3UO_4 corrected to 100 % theoretical density.

heat capacity data in [17] and was corrected to 100 % th.d. which gives λ_0 = 1.2 W/m·K at 20 °C and λ_0 = 0.6 W/m·K at 600 °C. However, these data are lower than those reported in [15,18], and should be disregarded.

The thermal conductivity of $Na_3(U,Pu)O_4$ was estimated from irradiation experiments of breached mixed oxide pins with different burnups (3 to 9 at.%) and linear heat ratings (26 to 33 kW/m) [36]. The thermal conductivity of 100 % dense $Na_3U_{1-y}Pu_yO_4$ falls between 0.9 and 1.0 W/m·K in the temperature range of 550 to 1100 °C.

Diffusion

The kinetics of the $Na_3U_{1-y}Pu_yO_4$ layer formation between $U_{1-y}Pu_yO_{2-x}$ and sodium was investigated between 873 and 1173 K in out-of-pile experiments [21,22,23] and in in-pile experiments [24]. The activation energy of the layer formation was reported as Q = 167 kJ/mol [21]. The rate determining step for this reaction is probably the diffusion of sodium through the formed $Na_3U_{1-y}Pu_yO_4$. The layer thickness d and the reaction time t in the different experiments is used for the calculation of the chemical diffusion coefficient $\bar{D} = d^2/2t$ of Na in $Na_3U_{1-y}Pu_yO_4$: $\bar{D}_{Na} = 3\cdot10^{-16} - 3\cdot10^{-15}$ m²/s at 873 K [22]; $\bar{D}_{Na} = 2\cdot10^{-14}$ at

1073 K [24]; $\bar{D}_{Na}$ = 10^{-11} m^2/s at 1473 K [21]. These data yield a chemical diffusion coefficient of Na in $Na_3U_{1-y}Pu_yO_4$, $\bar{D}_{Na}$ = $5 \cdot 10^{-6}$ exp(- Q/RT) m^2/s with an activation energy Q = 166 kJ/mol between 800 and 1500 K. This value is in good agreement with that in [21]. The chemical diffusion coefficient of Na in $Na_3U_{1-y}Pu_yO_4$ as a function of the inverse temperature is illustrated in fig. 13. It is supposed that the activation energy for the diffusion of sodium in $Na_3U_{1-y}Pu_yO_4$ is independent of the Pu/(U + Pu) ratio [21], hence the relationship should be valid also for the diffusion of Na in Na_3UO_4. Further kinetic experiments were reported on the volume expansion of $U_{0.7}Pu_{0.3}O_2$ pellets after reaction with sodium between 923 and 1073 K [46]. A value of 335 kJ/mol was determined for the apparent activation energy of the integral swelling.

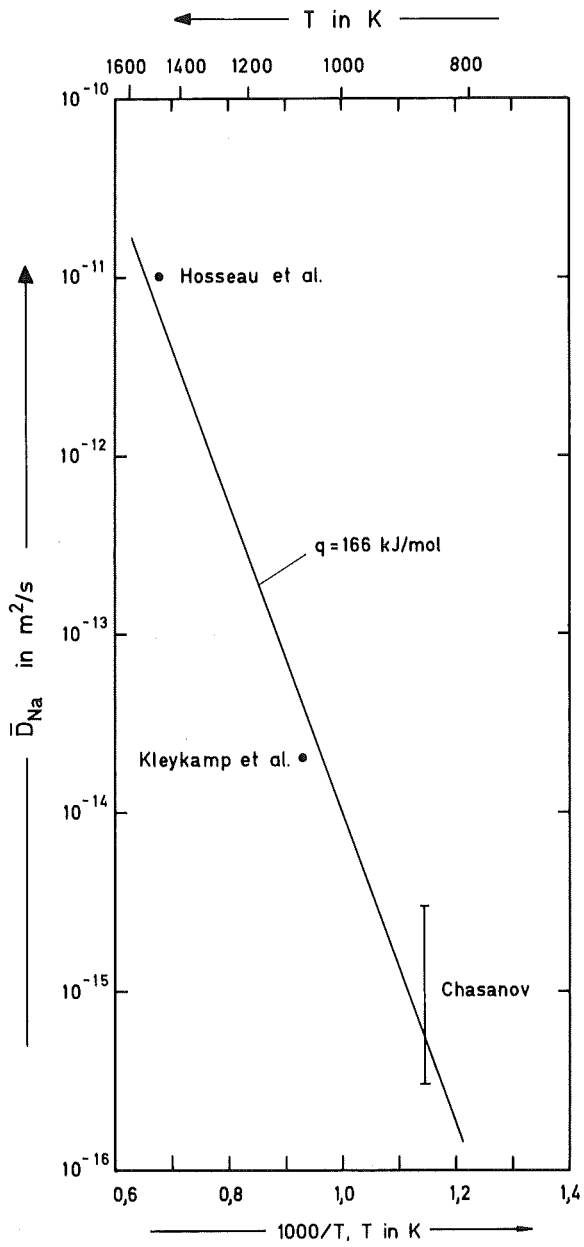

Fig. 13: Chemical diffusion coefficient $\bar{D}_{Na}$ of Na in $Na_3(U,Pu)O_4$.

3.6 Optical properties

Na_3UO_4 is chocolate-brown [8]; $NaUO_3$ is brown-violet [25] and red-brown [26], resp.; $Na_2U_2O_7$ is yellow-orange [11]; β-Na_4UO_5 is salmon-coloured [9]; α-Na_4UO_5 is dark red [9]; β-Na_2UO_4 is pink [9]; α-Na_2UO_4 is orange [9]; $Na_6U_7O_{24}$ is dark yellow [9]. Na_6PuO_6 is black [38,39]; β-Na_4PuO_5 is light brown [38,39]; α-Na_4PuO_5 is dark violet [38,39].

3.7 Chemical properties

Na_3UO_4 is hygroscopic in air yielding uranium oxide hydrate [8] or ultimately $Na_2U_2O_7$ [11]. $NaUO_3$ is stable against air, water and diluted acids [25]. Na_2UO_4 hydrolizes according to the reaction $Na_2UO_4 + H_2O \rightarrow Na_2U_2O_7 + NaOH$ [25]. $Na_2U_2O_7$ is the only stable phase in air up to 1300 °C [11].

Na_3PuO_4 and the other plutonates are stable in air but decompose by hydrolysis in wet atmospheres [38,39]. Na_6PuO_6 decomposes at 750 °C into β-Na_4PuO_5 which decomposes at 900 °C into Na_3PuO_4; this phase decomposes at 1000 °C into PuO_2 [39]. α-Na_4PuO_5 transforms at 500 °C into β-Na_4PuO_5 [39].

4. References

[1] J.P. Maupré, CEA-R-4905 (1978)

[2] J.D. Noden, J. Brit. Nucl. Energy Soc. 12 (1973) 57, 329

[3] A.W. Thorley in R.G. Taylor, R. Thompson, J. Nucl. Mater 115 (1983) 25

[4] D.R. Fredrickson, M.G. Chasanov, J. Chem. Thermodyn. 5 (1973) 485

[5] P.E. Blackburn, A.E. Martin, J.E. Battles, P.A.G. O'Hare, W.N. Hubbard, Proc. Fast Reactor Fuel Element Technol., New Orleans, USA, 1971 p. 479

[6] J.E. Battles, W.A. Shinn, P.E. Blackburn, J. Chem. Thermodyn. 4 (1972) 425

[7] R.T. Pepper, J.R. Stubbles, C.R. Tottle, Appl. Mater. Res. 3 (1964) 203

[8] H. Gläser, Thesis, Univ. Karlsruhe (1961); R. Scholder, H. Gläser, Z. anorg. allgem. Chemie 327 (1964) 15

[9] Landolt-Börnstein, Numerical Data and Functional Relationships in Science and Technology, N.S. Vol. III/7/e, Springer, 1976

[10] J.P. Marcon, O. Pesme, M. de Franco, Rev. Int. Hautes Temp. Réfr. 9 (1972) 193

[11] E.H.P. Cordfunke, B.O. Loopstra, J. Inorg. Nucl. Chem. 33 (1971) 2427

[12] S.F. Bartram, R.G. Fryxell, J. Inorg. Nucl. Chem. 32 (1970) 3701

[13] R. Lorenzelli, T. Athanassiadis, R. Pascard, J. Nucl. Mater. 130 (1985) 298

[14] O. Götzmann, K.H. Kurz, unpublished report (1982)

[15] G.L. Hofman, J.H. Bottcher, J.A. Buzzell, G.M. Schwarzenberger, J. Nucl. Mater. 139 (1986) 151

[16] D.W. Osborne, H.E. Flotow, J. Chem. Thermodyn. 4 (1972) 411

[17] D.R. Fredrickson, M.G. Chasanov, J. Chem. Thermodyn. 4 (1972) 419

[18] B. Schulz, J. Nucl. Mater. 114 (1983) 208

[19] J.H. Heuvel, unpublished report (1983)

[20] J.H. Heuvel, unpublished report (1985)

[21] M. Housseau, D. Déan, J.P. Marcon, J.F. Marin, CEA-N-1588 (1973)

[22] M.G. Chasanov, ANL-RDP-6 (1972), p. 5.8

[23] M. Housseau, J.F. Marin, F. Anselin, G. Déan, Fuel and Fuel Elements for Fast Reactors, Brussels, 1973, vol. 1, p. 271

[24] H. Kleykamp, H.D. Gottschalg, R. Fritzen, H. Späte, F. Bauer, unpublished report (1978)

[25] W. Rüdorff, H. Leutner, Z. anorg. allgem. Chemie 292 (1957) 193

[26] S. Kemmler-Sack, W. Rüdorff, Z. anorg. allgem. Chemie 354 (1967) 255

[27] P.A.G. O'Hare, W.A. Shinn, F.C. Mrazek, A.E. Martin, J. Chem. Thermodyn. 4 (1972) 401

[28] J.E. Battles, W.A. Shinn, P.E. Blackburn, J. Chem. Thermodyn. 4 (1972) 425

[29] M.G. Adamson, M.A. Mignanelli, P.E. Potter, M.H. Rand, J. Nucl. Mater. 97 (1981) 203

[30] P.A.G. O'Hare, H.R. Hoekstra, J. Chem. Thermodyn. 5 (1973) 769

[31] D.W. Osborne, H.E. Flotow, R.D. Dallinger, H.R. Hoekstra, J. Chem. Thermodyn. 6 (1974) 751

[32] P.A.G. O'Hare, H.R. Hoekstra, J. Chem. Thermodyn. 6 (1974) 965

[33] P.A.G. O'Hare, H.R. Hoekstra, D.R. Fredrickson, J. Chem. Thermodyn. 8 (1976) 255

[34] W.G. Lyon, D.W. Osborne, H.E. Flotow, H.R. Hoekstra, J. Chem. Thermodyn. 9 (1977) 201

[35] E.H.P. Cordfunke, R.P. Muis, W. Ouweltjes, H.E. Flotow, P.A.G. O'Hare, J. Chem. Thermodyn. 14 (1982) 313

[36] M.J. Lee, J.D.B. Lambert, S. Ukai, T. Odo, Trans. ANS 55 (1987) 294

[37] W. Dienst, K.H. Kurz, unpublished report (1985)

[38] C. Keller, L. Koch, K.H. Walter, J. Inorg. Nucl. Chem. 27 (1965) 1205

[39] C. Keller, L. Koch, K.H. Walter, J. Inorg. Nucl. Chem. 27 (1965) 1225

[40] C. Keller, KfK-225 (1964)

[41] M.A. Mignanelli, P.E. Potter, J. Nucl. Mater. 130 (1985) 289

[42] R.L. Eichelberger, AI-AEC-12685 (1968)

[43] J.S. Hislop, R. Thompson, D.A. Wood, AERE-M-3097 (1980)

[44] S. Pillon, Thesis, Univ. du Languedoc (1989), CEA-R-5489 (1989)

[45] E.H.P. Cordfunke, R.J.M. Konings, G. Prins, P.E. Potter, M.H. Rand, report ETSN-0005-NL (1988)

[46] M.A. Mignanelli, P.E. Potter, J. Nucl. Mater. 125 (1984) 182

[47] A.W. Thorley, NRL-R-1043 (R) (1989)

[48] E.H.P. Cordfunke, P.A.G. O'Hare, The Chem. Thermodyn. Actinide Elements Compds., Part 3, IAEA, Vienna, 1978

[49] O. Götzmann, personal commun. (1990)

[50] A.M. Chippindale, P.G. Dickens, W.T.A. Harrison, J. Solid State Chem. 78 (1989) 256